PHYSICAL REVIEW A VOLUME 58, NUMBER 2 AUGUST 1998

Multiphoton ac Stark effect in a bichromatically driven two-level atom

T. G. Rudolph,[1] H. S. Freedhoff,[1] and Z. Ficek[2]
[1]*Department of Physics and Astronomy, York University, 4700 Keele Street, Toronto, Ontario, Canada M3J 1P3*
[2]*Department of Physics and Centre for Laser Science, The University of Queensland, Brisbane, Australia 4072*
(Received 4 December 1997; revised manuscript received 6 April 1998)

We study the interaction of a two-level atom with two lasers of different frequencies and amplitudes: a strong laser of Rabi frequency $2\Omega_1$ on resonance with the atomic transition, and a weaker laser detuned by subharmonics $(2\Omega_1/n)$ of the Rabi frequency of the first. We find that under these conditions the second laser couples the dressed states created by the first in an n-photon process, resulting in ''doubly dressed'' states and in a ''multiphoton ac Stark'' effect. We calculate the eigenstates of the doubly dressed atom and their energies, and illustrate the role of this multiphoton ac Stark effect in its fluorescence, absorption, and Autler-Townes spectra. [S1050-2947(98)07607-0]

PACS number(s): 42.50.Hz, 32.80.−t

I. INTRODUCTION

The interaction of a two-level atom with an intense, nearly resonant laser field is of fundamental interest in atomic spectroscopy and quantum optics and has been studied extensively for over 25 years. Early interest focused on the atom driven by an intense monochromatic field and the resulting ''dressed'' system probed by a weak field. Fluorescence by the system was first predicted [1] and then observed [2], as was the absorption and dispersion by the entangled atom+driving field system of a weak probe field nearly resonant with either the driven transition [3] or the transition from a driven level to a third atomic level (Autler-Townes effect) [4].

Another area of interest involves the atomic response to amplitude-modulated (AM) and bichromatic driving fields. A 100% amplitude-modulated field is equivalent to a bichromatic field whose (mutually coherent) components have equal intensities, and whose frequencies are separated by twice the modulation frequency. Various aspects of this problem have been studied. For example, the fluorescence spectrum of an atom driven by a bichromatic field of equal amplitudes (Rabi frequencies) was observed [5] and interpreted using a dressed-atom analysis [6]. Since then a wide variety of studies have been performed on the fluorescence, near-resonant absorption, and Autler-Townes absorption of bichromatically driven atoms for both equal [7] and unequal [8] Rabi frequencies, and for average driving field frequency both tuned to and detuned from the atomic resonance [9,10].

Much attention has focused, in these studies, on the appearance of the ''subharmonic resonances'' displayed by the absorption spectrum of a strong probe beam monitoring a strongly driven two-level system [10–13]. The experimental data collected to date relating to the subharmonic absorption maxima of the strong probe also correspond to a study of the maxima of the integrated intensity of fluorescence by the atom when one component of the driving field (the ''pump'') is fixed in its frequency and intensity, while the frequency and/or intensity of the second component (the ''probe'') is varied. The connection of these subharmonic resonances with multiphoton gain has also been explored [14], and a two-photon optical lasing has been observed [15]. However, a ''strong probe'' is an intense field that itself alters the characteristics of the system it is supposed to be probing. Based on this observation, we therefore consider this system from the point of view that both laser fields ''dress'' the atom and analyze the energy states of the resulting system. We will show that the system is both in principle and in practice more profitably regarded in the context of this bichromatic excitation.

In the studies of resonance fluorescence from two- or three-level atoms under bichromatic excitation, both driving fields couple to the same atomic transition. In the related studies of multilevel atoms driven by n coherent laser fields each of the fields couples to only one of the n possible one-photon transitions [16]; in this latter case a multiphoton absorption is possible, but the driving fields can lead to only a ''one-photon ac Stark effect.'' In this paper we study a system in which two fields drive the same atomic one-photon transition, yet nevertheless the second field can couple to multiphoton resonances between dressed states of the first field. We find a new physical phenomenon: the splitting of the dressed states is due to an n-photon coupling between them, i.e., it represents an n-photon ac Stark effect. We present the fundamental dynamics of this system by examining the fluorescence spectrum, as well as the weak probe absorption and Autler-Townes spectra. We focus on the driving of the singly dressed system by a laser field tuned to the subharmonic resonances, and use the dressed-atom model both to explain the physical origin of novel spectral effects and to demonstrate that far more detailed information is in fact obtainable by suitable probing. The calculated fluorescence, probe absorption, and Autler-Townes spectra are extremely rich in detail, containing multiplets at the subharmonic as well as harmonic resonance frequencies with an intricate dependence on the order n of the resonance and on the relative Rabi frequencies of the driving field components.

In principle it is possible to write down and numerically solve the master equation or the Bloch equations of the system including all of these effects; this does not, however, lead to a physical understanding of the problem. In order to gain insight into the dynamics of the system, we use the ''dressed atom'' model for our bichromatically driven atom [19]. The energy levels of the entangled system of

atom+driving fields (i.e., the doubly dressed atom) are calculated first in Secs. II and III. Resonance fluorescence appears in this picture as a spontaneous emission cascade by the dressed atom down its ladder of energy manifolds. The absorption spectrum is interpreted as the net difference between absorption and stimulated emission of a weak, quasiresonant probe between the manifold sublevels, while the Autler-Townes spectrum reflects the net absorption from the manifold sublevels of a weak probe tuned to a third atomic level. These spectra are calculated in Sec. IV. In Sec. V we briefly discuss the multiphoton Stark effect that occurs when the strong field is detuned and the weaker field is on resonance. In Sec. VI we summarize our results, in Appendix A present details of the perturbation calculations involved in the determination of the dressed states, and in Appendix B tabulate the transition rates which govern the intensities of the spectral components.

II. THE SYSTEM

We consider a two-level atom with ground state $|g\rangle$ and excited state $|e\rangle$ separated by a transition frequency ω_0 and connected by a transition dipole moment $\vec{\mu}$. The atom is driven by a bichromatic field with frequency components ω_1 and ω_2 and corresponding (on resonance) Rabi frequencies $2\Omega_1$ and $2\Omega_2$. The atom is also coupled to all other modes of the electromagnetic field, which are assumed to be initially in their vacuum states. This coupling leads to spontaneous emission with a rate Γ.

The time evolution of the atomic system can be described by the reduced atomic density operator ρ, which in the Schrödinger picture obeys the master equation ($\hbar=1$) [20]

$$\frac{\partial\rho}{\partial t}=-i[H,\rho]-\frac{\Gamma}{2}(S^+S^-\rho+\rho S^+S^--2S^-\rho S^+), \quad (1)$$

where $S^+(S^-)=|e\rangle\langle g|$ ($|g\rangle\langle e|$) is the usual atomic raising (lowering) operator. The Hamiltonian H is composed of five terms,

$$H=H_a+H_1+H_2+V_1+V_2, \quad (2)$$

where

$$H_a=\omega_0 S^z \quad (3)$$

is the Hamiltonian of the atom, and

$$H_i=\omega_i a_i^\dagger a_i, \quad i=1,2, \quad (4)$$

are the Hamiltonians of the driving field components. In Eqs. (3) and (4), $S^z=\frac{1}{2}(|e\rangle\langle e|-|g\rangle\langle g|)$ is the atomic inversion, and a_i ($a_i^\dagger$) are the annihilation (creation) operators for the driving field modes. The terms

$$V_i=g_i(a_i^\dagger S^-+S^+a_i), \quad i=1,2, \quad (5)$$

where g_i are the atom-field coupling constants, describe the interaction of the laser fields with the atom (in the rotating-wave approximation).

We begin by diagonalizing the Hamiltonian H to find the eigenstates (dressed states) of the combined atom+driving fields system. This approach is valid for

$$\omega_1, \quad \omega_2 \gg \Omega_1, \quad \Omega_2 > \Gamma. \quad (6)$$

We consider only the case of $\Omega_2=\alpha\Omega_1$ with $\alpha<1$, and we examine the effect of the second field perturbatively. Moreover, we limit our calculations to the case in which the first field is on resonance with the atomic transition, $\omega_1=\omega_0$, and the second field is detuned from resonance by an integer fraction of the first field's Rabi frequency, so that

$$\omega_2=\omega_0+\frac{2\Omega_1}{n}. \quad (7)$$

This corresponds to driving the system by the second field at one of the ''subharmonic resonances'' of the Rabi frequency of the first field. The case of $n=1$ has recently been examined both theoretically [21] and experimentally [22]. As we shall see the situation for $n=2,3,\ldots$ produces dramatically different results. An n-photon coupling between dressed states leads to the appearance of multiplet features at subharmonic as well as harmonic resonance frequencies in the spectra.

The diagonalization of H leads to the dressed states of the system and their energies. However, instead of performing the diagonalization of the total Hamiltonian by treating the driving fields as a single combined field, we first diagonalize the Hamiltonian $H_{da}=H_a+H_1+V_1$ and calculate the dressed states of the atom+resonant field system. Next we couple the resulting singly dressed atom to the off-resonant field and calculate the dressed states and their energies of this ''doubly dressed'' atom. The eigenstates of the Hamiltonian H_{da} satisfy the eigenvalue equation

$$H_{da}|N\pm\rangle=[N\omega_0\pm\Omega_1]|N\pm\rangle, \quad (8)$$

where

$$2\Omega_1=2g_1\sqrt{\langle N\rangle} \quad (9)$$

is the Rabi frequency of the resonant field,[1]

$$|N\pm\rangle=\frac{1}{\sqrt{2}}(|g,N\rangle\pm|e,N-1\rangle) \quad (10)$$

are the singly dressed states, and N is the number of photons in the resonant mode [19]. The singly dressed states form a ladder of doublets, as shown in Fig. 1(a), with adjacent doublets separated by ω_0, and intradoublet splitting $2\Omega_1$.

Next, we add the second field and find that the eigenstates of the combined system $H_{da}+H_2$ are degenerate doublets:

$$\begin{aligned}|(N+n-m)+,M-n+m\rangle&\equiv|a_m^n\rangle,\\ |(N-m)-,M+m\rangle&\equiv|b_m^n\rangle,\end{aligned} \quad (11)$$

with energies

[1] In the derivation of Eq. (8), we have ignored the variation of Ω_1 with N, on the basis that the resonant laser is in a large amplitude coherent state with an average number of photons $\langle N\rangle\gg1$.

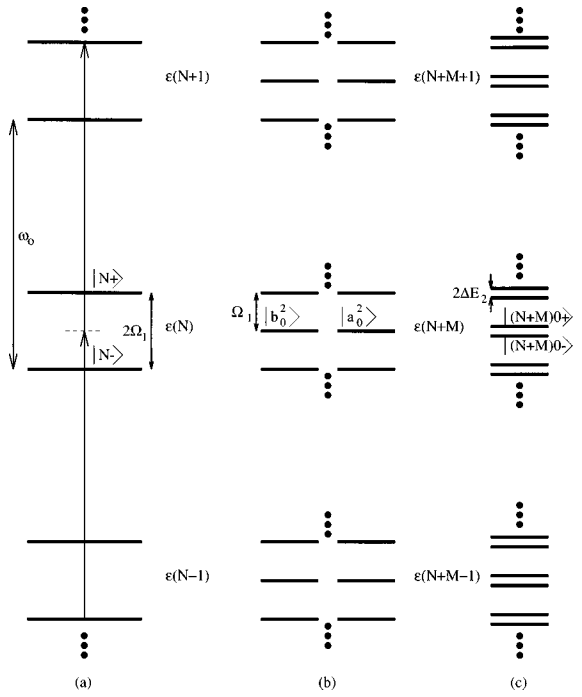

FIG. 1. (a) Energy levels of the singly dressed atom. Absorption of two laser 2 photons of frequency $\omega_2=\omega_0+\Omega_1$, corresponding to the case of $n=2$, is indicated by the arrows. (b) Energy levels of the singly dressed atom and laser 2 before the interaction between them is ''turned on.'' The energy manifolds each contain an infinite number of degenerate doublets with interdoublet separation Ω_1. (c) Addition of the interaction with laser 2 removes the degeneracy and leads to the splitting of the degenerate levels into doublets with an intradoublet separation $2\Delta E_2$.

$$E_{a_m}\equiv E_{b_m}=(N+M)\omega_0+\frac{\Omega_1}{n}[2(M+m)-n], \quad (12)$$

where M is the number of photons in the detuned mode 2. This degeneracy is due to an n-photon coupling between singly dressed states, as indicated for $n=2$ by arrows in Fig. 1(a). Thus, to this point, the energy structure of the system consists of an infinite number of manifolds (separated by ω_0), each containing an infinite number of degenerate doublets (separated by $2\Omega_1/n$), as shown in Fig. 1(b).

III. THE DOUBLY DRESSED STATES AND ENERGY SPLITTINGS

The addition of the interaction V_2 between the atom and field mode 2 removes the degeneracy between the states $|a_m^n\rangle$ and $|b_m^n\rangle$ and results in ''doubly dressed'' states. In order to show this, we diagonalize the Hamiltonian $H=H_{da}+H_2+V_2$ in the basis of the degenerate states $|a_m^n\rangle$ and $|b_m^n\rangle$. We perform the diagonalization using perturbation theory, and find that for $n=2,3,\ldots$ it is necessary to go to second-order degenerate perturbation theory to achieve this. This is due to the fact that the matrix elements $\langle\alpha|V_2|\beta\rangle$ $(\alpha,\beta=a,b)$ are zero, and the first nonvanishing perturbation calculations therefore involve diagonalization of the operator

$$\mathcal{R}^1\equiv\sum_{i\neq a,b}\frac{V_2|i\rangle\langle i|V_2}{E_a-E_i} \quad (13)$$

on the two-dimensional degenerate subspace $\{|a\rangle,|b\rangle\}$.

The details of the perturbation calculations are shown in Appendix A. After lengthy calculations, we find that the eigenstates of H are composed of nondegenerate doublets with splitting $2\Delta E_n$ [as shown in Fig. 1(c)], where ΔE_n, for $n=2$, 3, and 4, are given by the series expansions

$$\begin{aligned}\Delta E_2&=\Omega_1\sqrt{13}\left(\frac{1}{6}\alpha^2-\frac{493}{2808}\alpha^4+\frac{9123107}{52565760}\alpha^6+\cdots\right),\\ \Delta E_3&=\Omega_1\left(\frac{9}{32}\alpha^2+\frac{36117}{40960}\alpha^4-\frac{132460191}{26214400}\alpha^6+\cdots\right),\\ \Delta E_4&=\Omega_1\left(\frac{4}{15}\alpha^2+\frac{254}{3375}\alpha^4+\frac{9384656}{5315625}\alpha^6+\cdots\right).\end{aligned} \quad (14)$$

The corresponding eigenstates (the doubly dressed states), calculated as a perturbation expansion in α, are given by the following:

$n=2$:

$$\begin{aligned}|(N+M)m+\rangle=\mathcal{N}_2\Bigg\{&\eta|a\rangle+|b\rangle+\frac{1}{2}\alpha\left[-(\eta+1)|a_1\rangle+|b_1\rangle+\eta|a_{-1}\rangle+(\eta-1)|b_{-1}\rangle+\frac{1}{3}|a_3\rangle-\frac{1}{3}\eta|b_{-3}\rangle\right]+\frac{1}{12}\alpha^2\Bigg[\frac{-27}{52}(|a\rangle\\ &-\eta|b\rangle)+(3\eta-2)|a_2\rangle+|b_2\rangle+\eta|a_{-2}\rangle+(2\eta+3)|b_{-2}\rangle+\frac{1}{2}|a_4\rangle-\frac{1}{2}\eta|b_{-4}\rangle\Bigg]\Bigg\},\end{aligned}$$

$$\begin{aligned}|(N+M)m-\rangle=\mathcal{N}_2\Bigg\{&|a\rangle-\eta|b\rangle+\frac{1}{2}\alpha\left[(\eta-1)|a_1\rangle-\eta|b_1\rangle+|a_{-1}\rangle+(\eta+1)|b_{-1}\rangle-\frac{1}{3}\eta|a_3\rangle-\frac{1}{3}|b_{-3}\rangle\right]\\ &+\frac{1}{12}\alpha^2\Bigg[\frac{27}{52}(\eta|a\rangle+|b\rangle)+(3+2\eta)|a_2\rangle-\eta|b_2\rangle+|a_{-2}\rangle+(2-3\eta)|b_{-2}\rangle-\frac{1}{2}\eta|a_4\rangle-\frac{1}{2}|b_{-4}\rangle\Bigg]\Bigg\}, \quad (15)\end{aligned}$$

$n=3$:

$$|(N+M)m+\rangle=\mathcal{N}_3\Big\{|a\rangle+\frac{3}{4}\,\alpha\Big[\frac{3}{2}\,|b\rangle-|a_1\rangle+|a_{-1}\rangle+\frac{1}{2}\,|b_{-2}\rangle-\frac{1}{4}\,|b_{-4}\rangle\Big]$$
$$+\frac{27}{16}\,\alpha^2\Big[\frac{1}{2}\,|b_1\rangle-|b_{-1}\rangle+\frac{1}{8}\,|a_{-2}\rangle+\frac{7}{36}\,|b_{-3}\rangle+\frac{1}{8}\,|a_4\rangle-\frac{1}{20}\,|b_{-5}\rangle\Big]\Big\},$$
$$|(N+M)m-\rangle=\mathcal{N}_3\Big\{|b\rangle+\frac{3}{4}\,\alpha\Big[\frac{3}{2}\,|a\rangle+|b_1\rangle-|b_{-1}\rangle-\frac{1}{2}\,|a_2\rangle+\frac{1}{4}\,|a_4\rangle\Big]$$
$$+\frac{27}{16}\,\alpha^2\Big[|a_1\rangle-\frac{1}{2}\,|a_{-1}\rangle+\frac{1}{8}\,|b_2\rangle-\frac{7}{36}\,|a_3\rangle+\frac{1}{8}\,|b_{-4}\rangle+\frac{1}{20}\,|a_5\rangle\Big]\Big\}, \tag{16}$$

$n=4$:

$$|(N+M)m+\rangle=\mathcal{N}_4\Big\{|a\rangle+\alpha\Big[|a_{-1}\rangle-|a_1\rangle+\frac{1}{3}\,|b_{-3}\rangle-\frac{1}{5}\,|b_{-5}\rangle\Big]$$
$$+\alpha^2\Big[\frac{-5}{3}\,|b\rangle+\frac{2}{3}\,|a_2\rangle+\frac{2}{5}\,|a_{-2}\rangle-\frac{2}{3}\,|b_{-2}\rangle+\frac{7}{15}\,|b_{-4}\rangle-\frac{2}{15}\,|b_{-6}\rangle\Big]\Big\},$$
$$|(N+M)m-\rangle=\mathcal{N}_4\Big\{|b\rangle+\alpha\Big[|b_1\rangle-|b_{-1}\rangle-\frac{1}{3}\,|a_3\rangle+\frac{1}{5}\,|a_5\rangle\Big]+\alpha^2\Big[\frac{5}{3}\,|a\rangle+\frac{2}{3}\,|b_{-2}\rangle+\frac{2}{5}\,|b_2\rangle+\frac{2}{3}\,|a_2\rangle-\frac{7}{15}\,|a_4\rangle+\frac{2}{15}\,|a_6\rangle\Big]\Big\}, \tag{17}$$

where $\eta=-2/3-\sqrt{13}/3$, and $\mathcal{N}_2=[(1+\eta^2)(1+\frac{7}{9}\alpha^2)]^{-1/2}$, $\mathcal{N}_3=[1+\frac{484}{225}\alpha^2]^{-1/2}$, $\mathcal{N}_4=[1+\frac{657}{256}\alpha^2)]^{-1/2}$ are the normalization constants, and, for simplicity, we have introduced the notation $|a_i\rangle\equiv|a^n_{m+i}\rangle$, $|b_i\rangle\equiv|b^n_{m+i}\rangle$ for $i\neq 0$ and $|a_0\rangle=|a\rangle$, $|b_0\rangle=|b\rangle$.

We note the interesting effect that the perturbation V_2 lifts the degeneracy between the $|a\rangle$ and $|b\rangle$ states for all $n\geqslant 2$; however, a mixture of these states *to zeroth order in* α does not occur for $n>2$. To understand this we refer to the operator $\mathcal{R}^1$, whose diagonal elements represent the shift of the degenerate states due to their coupling, through V_2, with other states of the manifold. Since $\langle a|\mathcal{R}^1|a\rangle=-\langle b|\mathcal{R}^1|b\rangle\neq 0$ for all n, the states are always shifted in opposite directions, which lifts the degeneracy at second order. The off-diagonal elements of $\mathcal{R}^1$ represent a coupling *between* the degenerate states through the other states of the manifold. It is not difficult to show that for $n>2$ these off-diagonal elements are zero; hence the matrix representation of $\mathcal{R}^1$ is diagonal and no superposition of the states occurs until order α^{n-2}.

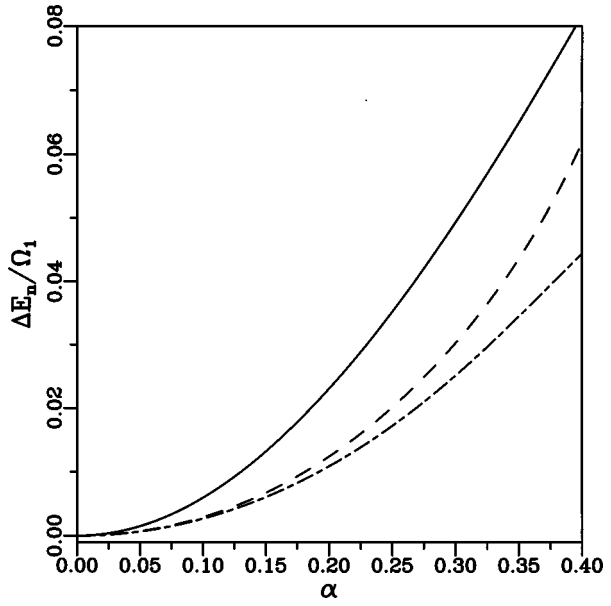

FIG. 2. The n-photon energy splitting $\Delta E_n/\Omega_1$, plotted as a function of α for $n=2$ (solid line), $n=3$ (dashed line), and $n=4$ (dashed-dotted line).

The splittings ΔE_n are plotted in Fig. 2 as a function of α. Clearly for small α the splittings exhibit a quadratic dependence on α, and decrease with increasing n. Moreover for $\alpha<0.1$ the splittings for $n=3$ and 4 are almost exactly equal. This is a consequence again of the fact that for $n\geqslant 3$ the states $|a\rangle$ and $|b\rangle$ do not couple to each other through $\mathcal{R}^1$, which results in the leading term of the expansion for ΔE_n rapidly approaching $\frac{1}{4}\Omega_1\alpha^2$ for large n. Thus as n increases, the small α behavior of the splittings becomes almost identical.

IV. THE FLUORESCENCE, WEAK PROBE, AND AUTLER-TOWNES ABSORPTION AND DISPERSION SPECTRA

A. Spectral frequencies and transition rates

The interaction between the atom and the vacuum modes of the electromagnetic field leads to a spontaneous emission cascade down the energy manifold ladder of the dressed atom. Transitions occur between any pair of dressed states with a probability proportional to the absolute square of the dipole transition moment connecting them. Using the dressed states (15)–(17) we find that the transitions from $|(N+M)m\sigma\rangle$ to $|(N+M-1)(m+j)\epsilon\rangle$ $(\epsilon,\sigma\in\{+,-\})$ occur at frequencies

$$\omega_j^{\pm\pm}=\omega_0-j\frac{2\Omega_1}{n} \tag{18}$$

and

$$\omega_j^{\pm\mp}=\omega_0-j\frac{2\Omega_1}{n}\pm 2\Delta E_n, \tag{19}$$

indicating that the fluorescence spectrum will consist of a series of triplets with intratriplet spacing $2\Delta E_n$ centered at integer multiples of $2\Omega_1/n$, i.e., at both subharmonics and superharmonics of the strong field Rabi frequency. Nonzero transition probabilities occur only between states within neighboring manifolds. The relevant transition rates are therefore of the form

$$\Gamma_j^{\sigma\epsilon}=\Gamma\left|\langle (N+M)m\sigma|S^+|(N+M-1)(m+j)\epsilon\rangle\right|^2. \tag{20}$$

These transition rates (normalized to Γ, as are all relevant results presented henceforth) are presented explicitly in Appendix B. In order to show the first nonvanishing terms in the transition rates, the calculations for $n=2$ are presented correct to order α^2, whereas for $n=3,4$ they are presented correct to order α^4.

B. Populations of the dressed states

We use the master equation (1) to find the time evolution of the populations of the doubly dressed states and of the coherences between them. To study the populations, we project the master equation onto $|(N+M)m\pm\rangle$ on the right and $\langle (N+M)m\pm|$ on the left. We make the secular approximation in which we ignore couplings between populations and coherences and introduce the ''reduced populations'' [19]

$$\Pi_m^{\pm}=\sum_{N,M}\langle (N+M)m\pm|\rho|(N+M)m\pm\rangle. \tag{21}$$

Because $N,M\gg 1$ we can also assume that the populations vary very slowly with m, and so

$$\Pi_m^{\pm}\simeq\Pi_{m\pm 1}^{\pm}\simeq\cdots\equiv\Pi^{\pm}. \tag{22}$$

The population equations then reduce to a pair of coupled equations

$$\dot{\Pi}^{\pm}=\mp A^+\Pi^+\pm A^-\Pi^-, \tag{23}$$

where the dot denotes differentiation with respect to Γt, and the coefficients $A^{\pm}$ are given by the following: For $n=2$:

$$A^{\pm}=\frac{35}{104}-\left(\frac{61}{24336}\pm\frac{\sqrt{13}}{12}\right)\alpha^2+\left(\frac{99556813}{455569920}\mp\frac{259\sqrt{13}}{2808}\right)\alpha^4. \tag{24}$$

For $n=3$:

$$A^+=\frac{1}{4}+\frac{381}{512}\alpha^2-\frac{4421529}{819200}\alpha^4, \qquad A^-=\frac{1}{4}-\frac{285}{512}\alpha^2-\frac{5538249}{819200}\alpha^4. \tag{25}$$

For $n=4$:

$$A^+=\frac{1}{4}+\frac{17}{225}\alpha^2+\frac{158051}{101250}\alpha^4, \qquad A^-=\frac{1}{4}-\frac{13}{225}\alpha^2+\frac{136931}{101250}\alpha^4. \tag{26}$$

The equations (23) have steady state solutions

$$\Pi_{ss}^{\pm}=\frac{A^{\mp}}{A^++A^-}, \tag{27}$$

which yield explicitly the following: For $n=2$:

$$\Pi_{ss}^{\pm}=\frac{1}{2}\mp\frac{13\sqrt{13}}{105}\alpha^2\pm\frac{4502\sqrt{13}}{33075}\alpha^4. \tag{28}$$

For $n=3$:

$$\Pi_{ss}^{\pm}=\frac{1}{2}\mp\frac{3}{16}\alpha^2\mp\frac{2241}{2560}\alpha^4. \tag{29}$$

For $n=4$:

$$\Pi_{ss}^{\pm}=\frac{1}{2}\mp\frac{2}{15}\alpha^2\mp\frac{688}{3375}\alpha^4. \tag{30}$$

In the case of resonant monochromatic excitation, the dressed states are equally populated (in the secular approximation). However, the atom still exhibits weak emissive and absorptive properties that arise from multiphoton processes [17,18]. In the case of bichromatic driving, however, the populations $\Pi_{ss}^{\pm}$ depend on α and are unequal even within the secular approximation. This results in first-order absorption and emission at all sideband frequencies, with central components that still vanish, because they correspond to $+\Leftrightarrow+$ and $-\Leftrightarrow-$ transitions (which involve equal upper and lower state populations). The difference between the populations depends intricately upon the strength of the second laser and decreases with increasing n, indicating a decreasing efficiency of the second laser. The effective Rabi frequency of the second laser decreases with increasing n, as the laser drives the higher-order resonances.

C. Coherences and spectral linewidths

All spectra of the system are related to the time evolution of the atomic dipole moment operator S^+ given by

$$S^+=\sum_{\substack{l\epsilon,m\sigma\\N,M}}S^+_{l\epsilon,m\sigma}\rho^{(+)}_{l\epsilon,m\sigma,N,M}, \tag{31}$$

where $S^+_{l\epsilon,m\sigma}=\langle (N+M)l\epsilon|S^+|(N+M-1)m\sigma\rangle$, and

$$\rho^{(+)}_{l\epsilon,m\sigma,N,M}=|(N+M)l\epsilon\rangle\langle (N+M-1)m\sigma|. \tag{32}$$

The matrix elements of the off diagonal operators (32) represent coherences between the dressed states, and these oscillate at frequencies (18) and (19).

First, we consider transitions at the frequencies of the sidebands of each triplet (19). For values of Ω_1 and Ω_2 corresponding to the range (6), it is easily verified that the spectral lines are all nonoverlapping. The equations of motion of the corresponding density matrix elements are therefore uncoupled and from the master equation (1) we find that they are given by

$$\dot{\rho}_{l\pm,m\mp,N,M} = -(i\omega_{l-m}^{\pm\mp} + \Gamma_s)\rho_{l\pm,m\mp,N,M}, \tag{33}$$

where the linewidths Γ_s are as follows. For $n=2$:

$$\Gamma_s = \frac{69}{104} + \frac{61}{24336}\,\alpha^2 + \frac{99556813}{227784960}\,\alpha^4.$$

For $n=3$:

$$\Gamma_s = \frac{3}{4} - \frac{333}{512}\,\alpha^2 + \frac{4979889}{819200}\,\alpha^4. \tag{34}$$

For $n=4$:

$$\Gamma_s = \frac{3}{4} - \frac{2}{225}\,\alpha^2 - \frac{147491}{101250}\,\alpha^4.$$

Next we consider the transitions at the central component of each triplet. In this case the two matrix elements $\rho^{(+)}_{l+,m+,N,M}$ and $\rho^{(+)}_{l-,m-,N,M}$ oscillate at the same frequency (18), and therefore have coupled equations of motion. When we average over the driving field, the reduced coherences $\rho^{(+)}_{l\pm,m\pm} = \Sigma_{NM}\rho^{(+)}_{l\pm,m\pm,N,M}$ are found to obey the same coupled equations of motion as do the populations $\Pi^{\pm}$, with the addition in each of the freely oscillating terms $-i\omega^{\pm\pm}_{l-m}\rho^{(+)}_{l\pm,m\pm}$, given by

$$\dot{\rho}_{l\pm,m\pm} = -(i\omega^{\pm\pm}_{l-m} + A^{\pm})\rho_{l\pm,m\pm} + A^{\mp}\rho_{l\mp,m\mp}. \tag{35}$$

The associated dipole moments $p^{(+)}_{l\pm,m\pm} = S^{+}_{l\pm,m\pm}\rho^{(+)}_{l\pm,m\pm}$ then obey the equations

$$\dot{p}^{(+)}_{l\pm,m\pm}(t) = -(i\omega^{\pm\pm}_{l-m} + A^{\pm})p^{(+)}_{l\pm,m\pm}(t) - A^{\mp}p^{(+)}_{l\mp,m\mp}(t), \tag{36}$$

whose solutions are readily found to be

$$p^{(+)}_{l\pm,m\pm}(t) = \frac{\pm u_1}{\sqrt{(A^+)^2 + (A^-)^2}}A^{\mp}e^{-i\omega^{\pm\pm}_{l-m}t} + u_2 e^{-(i\omega^{\pm\pm}_{l-m} + \Gamma_c)t}, \tag{37}$$

where the constants u_1 and u_2 can be found from initial conditions. We do not, however, require the values of u_1 and u_2 in order to calculate the spectra and therefore do not solve for them. The first term in Eq. (37) corresponds to the elastic components, while the second term corresponds to the inelastic central components at frequencies $\omega^{\pm\pm}_{l-m}$ with linewidth given by

$$\Gamma_c = A^+ + A^-. \tag{38}$$

For all n we find $\Gamma_c = 2(1-\Gamma_s)$. We see from Eqs. (34) and (38) that the spectral linewidths depend on α such that the linewidths of the sideband components of the triplets decrease with increasing n, whereas the linewidths of the central components increase with increasing n.

D. Fluorescence spectrum

The fluorescence spectrum is given by the real part of the Fourier transform of the correlation function of the dipole-moment operator $\langle p^{(+)}(t)p^{(-)}(t')\rangle$, $t>t'$. From the quantum regression theorem [24], it is well known that for $t>t'$ the two-time average $\langle p^{(+)}_{l\epsilon,m\sigma}(t)p^{(-)}(t')\rangle$ satisfies the same equation of motion as the one-time average $\langle p^{(+)}_{l\epsilon,m\sigma}(t)\rangle$, with the initial conditions

$$\langle p^{(+)}_{l\epsilon,m\sigma}(t')p^{(-)}(t')\rangle = \Gamma^{\epsilon\sigma}_{l-m}\Pi^{\epsilon}_{ss}, \tag{39}$$

where $\Gamma^{\epsilon\sigma}_{l-m}$ are the transition rates given by Eqs. (B1)–(B3), and Π^{ϵ}_{ss} are the steady-state populations of the dressed states given by Eq. (28). The equations of motion for the one-time averages $\langle p^{(+)}_{l\epsilon,m\sigma}(t)\rangle$ were obtained in Sec. IV C. Thus, in the limit of large Ω_2 $(\Omega_2 > \Gamma)$, where the spectral lines do not overlap, the fluorescence spectrum (apart from geometrical and atomic factors) is given by

$$S(\omega) = \sum_{j=-\infty}^{\infty}\left(\frac{\Gamma_j^{+-}\Pi^{+}_{ss}\Gamma_s}{(\omega-\omega_j^{+-})^2+\Gamma_s^2} + \frac{\Gamma_j^{-+}\Pi^{-}_{ss}\Gamma_s}{(\omega-\omega_j^{-+})^2+\Gamma_s^2} + \frac{(\Gamma_j^{++}\Pi^{+}_{ss}+\Gamma_j^{--}\Pi^{-}_{ss})\Gamma_c}{(\omega-\omega_j^{++})^2+\Gamma_c^2}\right), \tag{40}$$

where the sum over j indicates a sum over the nonvanishing transitions as given by Eqs. (B1)–(B3). In Fig. 3 we plot this analytical expression for the fluorescence spectrum for $n=2$, 3, and 4.[2] The arrow in the diagram indicates the frequency of the second field. It is seen that for all n the spectrum consists of a series of triplets with intertriplet spacing $2\Omega_1/n$ and intratriplet spacing $2\Delta E_n$. With increasing n, the number of triplets increases while the splitting of each triplet decreases. The structure of the spectrum reveals the presence of both the multiphoton transitions (in the appearance of the subharmonic and harmonic features) and the multiphoton ac Stark effect (in the intratriplet splitting).

E. Weak probe nearly resonant with ω_0: absorption and dispersion

It is interesting to consider as well the absorption and dispersion of a weak beam probing the doubly dressed atom. Since the dressed states are unequally populated, the absorption spectrum can give information about population inversions between the dressed states. The absorption and disper-

[2]We note here that we have solved the master equation (1) numerically and have found that in order to get excellent agreement between the numerical and the present analytical results, we have to extend the dressed atom calculations to order α^6. Therefore, all the spectra plotted here include the populations and transition rates correct to α^6.

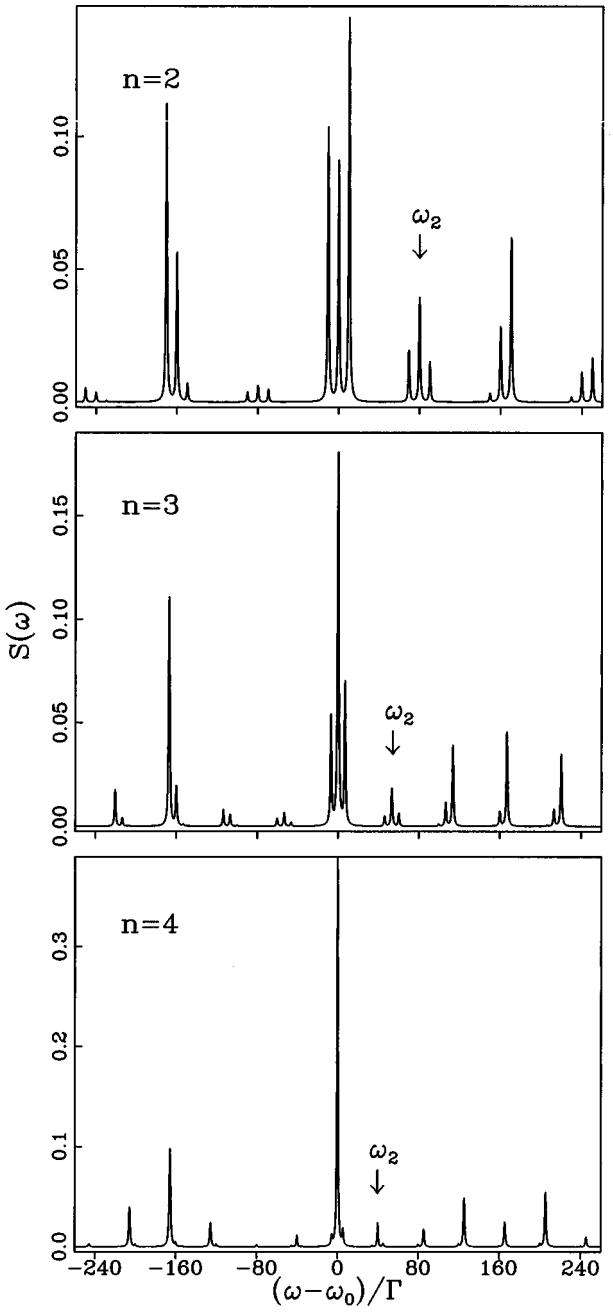

FIG. 3. The fluorescence spectrum for $2\Omega_1=160\Gamma$, $\alpha=0.35$, and different n: (a) $n=2$, (b) $n=3$, (c) $n=4$.

sion profiles of a weak probe beam of frequency ω_p are given by the real and imaginary parts, respectively, of the Fourier transform of the commutator $\langle[S^-(t),S^+(t')]\rangle$. The term $\langle S^-(t)S^+(t')\rangle$ of the commutator is associated with absorption and the term $\langle S^+(t')S^-(t)\rangle$ with stimulated emission of the probe beam. From the quantum regression theorem [24], it is well known that for $t>t'$ the two-time commutator $\langle[S^-_{l\epsilon,m\sigma}(t),S^+(t')]\rangle$ satisfies the same equation of motion as does the density matrix element $[\rho^{(+)}_{l\epsilon,m\sigma}(t)]^*$, with the initial condition

$$\langle[S^-_{l\epsilon,m\sigma}(t'),S^+(t')]\rangle=\Gamma^{\epsilon\sigma}_{l-m}(\Pi^{\epsilon}_{ss}-\Pi^{\sigma}_{ss}). \tag{41}$$

Thus, it is straightforward to show that in the case of non-overlapping spectral components the absorption spectrum of a probe beam nearly resonant with the atomic transition frequency is given by

$$W(\omega_p)=\sum_{j=-\infty}^{\infty}\left(\frac{\Gamma_j^{+-}(\Pi^-_{ss}-\Pi^+_{ss})\Gamma_s}{(\omega_p-\omega_j^{+-})^2+\Gamma_s^2}+\frac{\Gamma_j^{-+}(\Pi^+_{ss}-\Pi^-_{ss})\Gamma_s}{(\omega_p-\omega_j^{-+})^2+\Gamma_s^2}\right), \tag{42}$$

and the dispersion profile by

$$D(\omega_p)=\sum_{j=-\infty}^{\infty}\left(\frac{\Gamma_j^{+-}(\Pi^-_{ss}-\Pi^+_{ss})(\omega_p-\omega_j^{+-})}{(\omega_p-\omega_j^{+-})^2+\Gamma_s^2}+\frac{\Gamma_j^{-+}(\Pi^+_{ss}-\Pi^-_{ss})(\omega_p-\omega_j^{-+})}{(\omega_p-\omega_j^{-+})^2+\Gamma_s^2}\right). \tag{43}$$

The expressions (42) and (43) are plotted respectively in Figs. 4 and 5. They contain features at the same frequencies and with the same linewidths as their counterparts in $S(\omega)$, but with widely differing intensities depending on α. As the calculations have been made within the secular approximation, there are no (small) central features in the components of the absorption spectra. Therefore the absorption spectrum and the dispersion profile are composed of doublets centered at the frequencies $\omega_j^{\pm\mp}$. In each doublet of the absorption spectrum one sideband is absorbing and the other amplifying depending on the difference in steady-state populations of the lower and upper levels of the transition. It is interesting to note from Fig. 4 that with increasing n the maximum of amplification and absorption shifts from the central doublet to the Rabi sidebands. The same occurs with the dispersion, as seen in Fig. 5. Moreover, as n increases the red features become exclusively emissive whereas the blue features become only absorptive. The amplification at frequencies smaller than ω_0 is relatively large compared to the absorption at frequencies greater than ω_0, in contrast with the monochromatic case, where the amplification at one of the sidebands is always small compared to the absorption at the other sideband [3].

The dispersion, shown in Fig. 5, also exhibits interesting modifications. For example, in the region between the central doublet there is a strong negative dispersion with minimal absorption. For $n=2$, this effect is also seen in all harmonic and subharmonic doublets. With increasing n the negative dispersion decreases in the harmonic and subharmonic doublets whereas the central structure is remarkably stable against variation in n.

It should be emphasized here that this system may prove useful in the production of optical materials having a large index of refraction accompanied by vanishing absorption [25]. An advantage of this system is that near the central frequency, where the absorption vanishes, both the absorption and dispersion change slowly with frequency. Therefore, our system is a convenient candidate for this experimental application, since it does not require a precise matching of the probe beam frequency to the point of vanishing absorption.

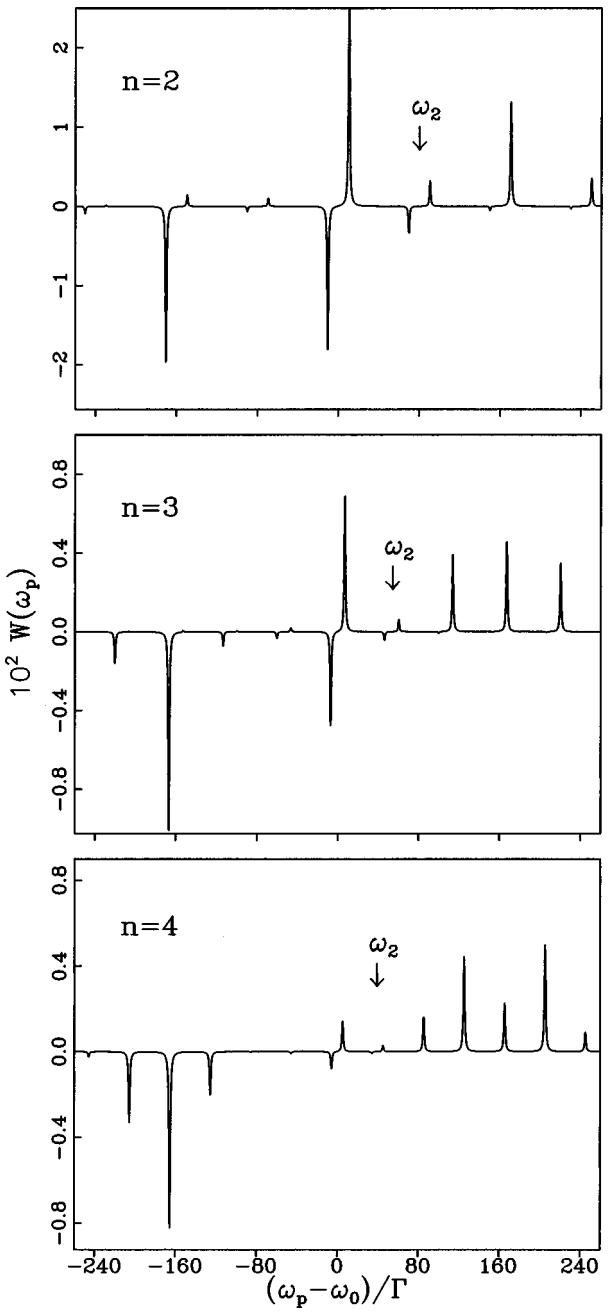

FIG. 4. The near-resonance absorption spectrum for the same parameters as in Fig. 3. (a) $n=2$, (b) $n=3$, (c) $n=4$.

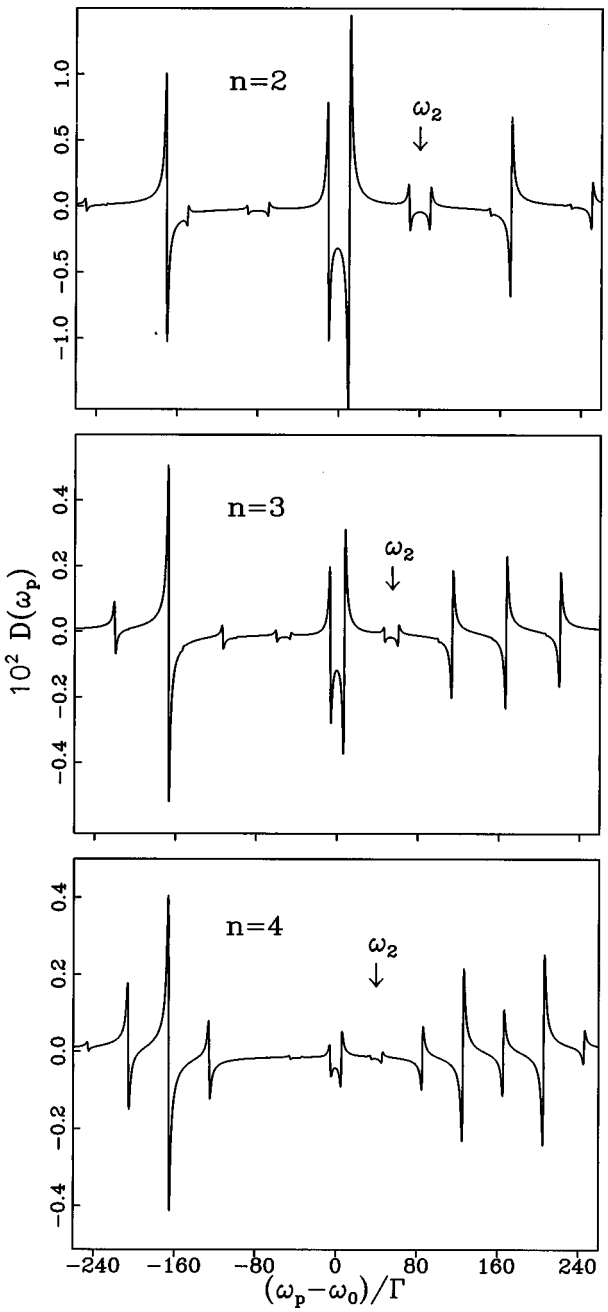

FIG. 5. The near-resonance dispersion profile for the same parameters as in Fig. 3. (a) $n=2$, (b) $n=3$, (c) $n=4$.

F. Autler-Townes absorption and dispersion profiles

The structure and properties of the doubly dressed atom can also be studied by monitoring the system with a weak probe beam coupled to a third (bare) atomic state. We assume that a third atomic level $|c\rangle$ is connected to $|g\rangle$ with a nonzero dipole moment, and with a transition frequency ω_c much different from ω_0. The transition is monitored by a weak probe beam of frequency ω_3 tuned close to ω_c. The intensity of the features corresponding to absorption from the dressed state $|(N+M)m\pm\rangle$ is proportional to the product of the steady-state population $\Pi_{ss}^{\pm}$ and the transition rate from $|(N+M)m\pm\rangle$ to $|c,N,M\rangle$, which itself is proportional to [19]

$$\Lambda_m^{\pm}=\Gamma_3|\langle(N+M)m\pm|g,N,M\rangle|^2, \tag{44}$$

where Γ_3 is the natural width of level $|c\rangle$. These quantities are readily evaluated using the dressed states (15)–(17) and are listed (normalized to Γ_3) in Appendix B. The frequencies at which the absorption occurs from $|(N+M)m\pm\rangle$ to $|c,N,M\rangle$ are given by

$$\omega_j^{\pm}=\omega_c-\left(\frac{2j}{n}-1\right)\Omega_1\mp\Delta E_n, \tag{45}$$

while the linewidths are given by

$$\Gamma_a=\frac{\Gamma_s+\Gamma_3/\Gamma}{2}. \tag{46}$$

Accordingly, the Autler-Townes absorption spectrum can be written as

$$A(\omega_3)=\sum_j\left(\frac{\Lambda_j^+\Pi_{ss}^+\Gamma_a}{(\omega_3-\omega_j^+)^2+\Gamma_a^2}+\frac{\Lambda_j^-\Pi_{ss}^-\Gamma_a}{(\omega_3-\omega_j^-)^2+\Gamma_a^2}\right), \tag{47}$$

and the corresponding dispersion profile is

$$T(\omega_3)=\sum_j\left(\frac{\Lambda_j^+\Pi_{ss}^+(\omega_3-\omega_j^+)}{(\omega_3-\omega_j^+)^2+\Gamma_a^2}+\frac{\Lambda_j^-\Pi_{ss}^-(\omega_3-\omega_j^-)}{(\omega_3-\omega_j^-)^2+\Gamma_a^2}\right). \tag{48}$$

In Figs. 6 and 7 we plot the Autler-Townes absorption and dispersion spectra, respectively, for the same parameters as in Fig. 3. Each consists of a series of doublets, located at frequencies $2m\Omega_1/n$, where $m=0,\pm1,\pm2,\ldots$ for n even and $m=\pm\frac{1}{2},\pm\frac{3}{2},\pm\frac{5}{2},\ldots$ for n odd. The intradoublet separation is $2\Delta E_n$. The most intense doublets are those centered at the frequencies $\omega_c\pm\Omega_1$, which correspond to the Autler-Townes frequencies of a monochromatically driven atom. The width of all lines is Γ_a, and once again an intricate dependence of the peak intensities on α is evident. Care must be taken when comparing the transition rates (B4) with the doublets in Fig. 6. The transition rates $\Lambda_0^{\pm}$ correspond to the sideband doublet at $\omega_3=\omega_c+\Omega_1$, not to the central one, whereas $\Lambda_i^{\pm}$ corresponds to the ith doublet to the left (right) of this intense doublet if i is positive (negative).

V. $\alpha>1$: STRONGER FIELD DETUNED, WEAKER ON RESONANCE

In this section, we consider briefly a role reversal of the driving fields, with the stronger detuned from ω_0 by an amount Δ, and the weaker field on resonance:

$$\omega_1=\omega_0,\quad \omega_2=\omega_0+\Delta, \tag{49}$$

$$\Omega_2=\alpha\Omega_1,\quad \alpha>1. \tag{50}$$

The atom can then be viewed as interacting first with the dominant field (of frequency ω_2), with an effective Rabi frequency

$$2G_2=\sqrt{\Delta^2+4\Omega_2^2}. \tag{51}$$

Whenever the detuning Δ is such that ω_1 lies at a subharmonic resonance of $2G_2$ ($\Delta=2G_2/n$), or alternatively, whenever the detuning and resonant Rabi frequency of field 2 are related by the equation

$$2\Omega_2=\Delta\sqrt{n^2-1},\quad n>1, \tag{52}$$

a multiphoton ac Stark effect again results. All the features described in the previous sections for $\alpha<1$ again appear, but centered in this case at frequencies ω_2 and $\omega_2\pm j(2G_2/n)$.

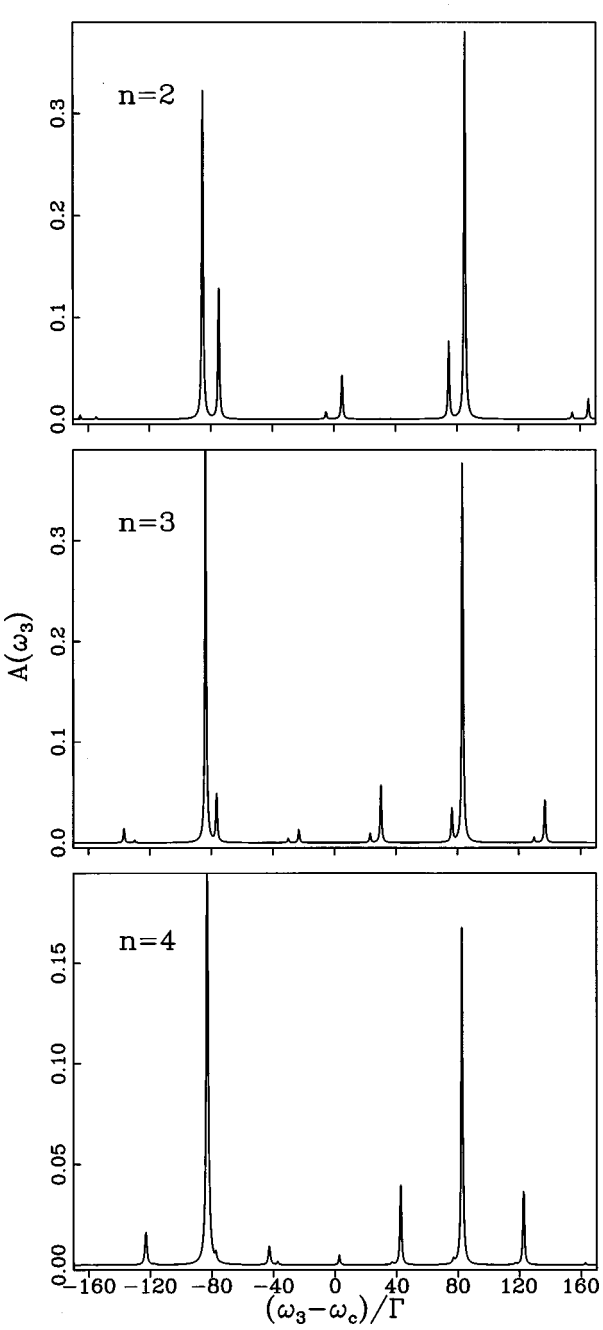

FIG. 6. The Autler-Townes absorption spectrum for the same parameters as in Fig. 3 and natural linewidth of the third level $\Gamma_3=\Gamma/3$. (a) $n=2$, (b) $n=3$, (c) $n=4$.

VI. CONCLUSIONS

We have studied the effect of bichromatic excitation on the radiative and absorptive properties of a two-level atom under the condition that one of the excitation fields is strong and exactly resonant with the atomic transition, while the other is weaker and detuned by a subharmonic of the Rabi frequency of the strong field. The energy levels of this system have been found and the radiative and absorptive properties interpreted in terms of the transitions between them. We have shown that this system, despite the one-photon coupling between the atom and driving fields, exhibits a multiphoton ac Stark effect. As such the fluorescence, absorption

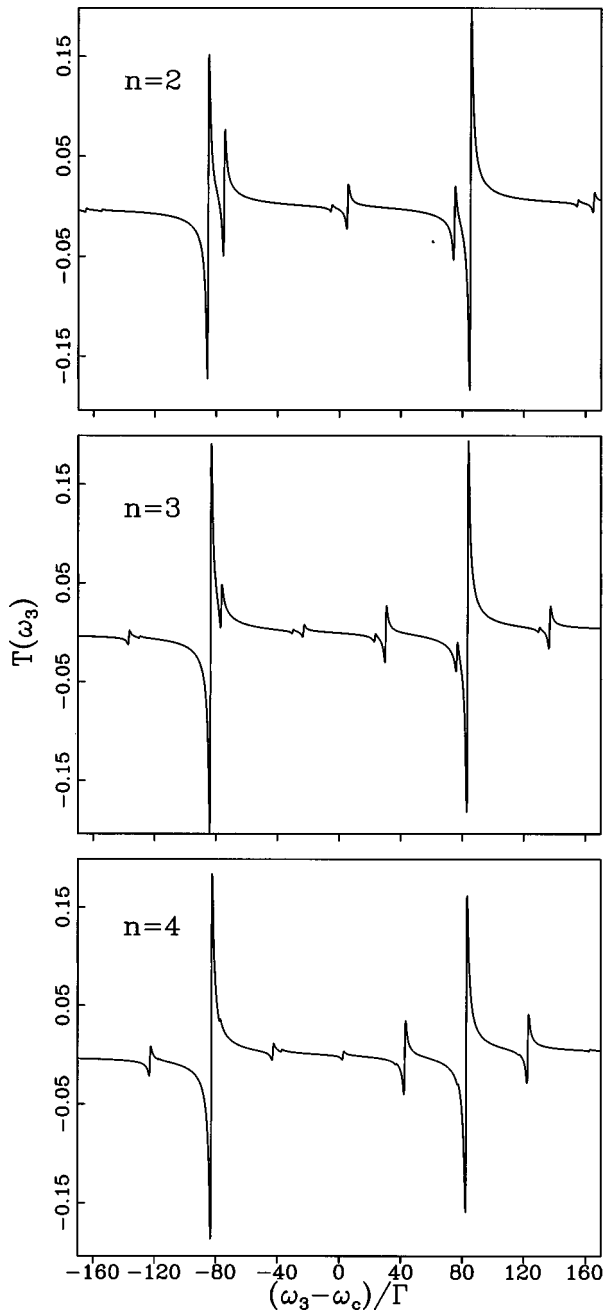

FIG. 7. The Autler-Townes dispersion profile for the same parameters as in Fig. 3 and natural linewidth of the third level $\Gamma_3=\Gamma/3$. (a) $n=2$, (b) $n=3$, (c) $n=4$.

and Autler-Townes spectra exhibit spectral features at subharmonics as well as harmonics of the Rabi frequency of the strong field, with the number of features dependent on the order n of the resonance. The presence of the multiphoton ac Stark effect leads to a splitting of each of the features of the fluorescence and near resonance absorption spectra into a triplet, and of the Autler-Townes spectrum into a doublet.

Finally, we would like to point out that the multiphoton splitting and the Autler-Townes spectra, of a system similar to that considered here, have recently been observed experimentally [23] and our theoretical predictions agree with these observations.

ACKNOWLEDGMENTS

We are grateful to Andrew Greentree, Neil Manson, and Changjiang Wei for sharing their experimental data with us prior to its publication. This research was supported in part by the Australian Research Council and by the Natural Sciences and Engineering Research Council of Canada, to whom the authors extend their thanks.

APPENDIX A: PERTURBATION THEORY FOR TWO DEGENERATE LEVELS

We consider a general perturbation λV of a Hamiltonian H_0 whose eigenvalues $E_1,E_2,\ldots$ and eigenstates $|1\rangle,|2\rangle,\ldots$ are known. In particular we consider the case when two of the unperturbed eigenstates $|a\rangle$ and $|b\rangle$ are degenerate with energy $E_a\equiv E_b$. In the standard manner we assume that the perturbed eigenstates and energies can be expanded as a power series in λ of the form

$$|\psi\rangle=|\psi\rangle^{(0)}+\lambda|\psi\rangle^{(1)}+\lambda^2|\psi\rangle^{(2)}+\cdots, \tag{A1}$$

$$E=E^0+\lambda E^{(1)}+\lambda^2E^{(2)}+\cdots, \tag{A2}$$

that the wave function correct to zero order is given by

$$|\psi\rangle^{(0)}=C_a^{(0)}|a\rangle+C_b^{(0)}|b\rangle \tag{A3}$$

and that the mth order correction to the wave function can be written as

$$|\psi\rangle^{(m)}=C_a^{(m)}|a\rangle+C_b^{(m)}|b\rangle+\sum_{i\neq a,b}C_i^{(m)}|i\rangle. \tag{A4}$$

The inclusion of the states $|a\rangle$ and $|b\rangle$ in the higher order corrections is often omitted in treatments of perturbation theory, but in fact is found to be critical to a correct calculation of the n-photon dynamic Stark effect discussed in this paper.

By substitution of these expressions into the Schrödinger equation, we set up a series of matrix equations of the form

$$G_0\mathbf{C}^{(0)}=E^{(1)}\mathbf{C}^{(0)}, \tag{A5}$$

$$G_0\mathbf{C}^{(1)}+G_1\mathbf{C}^{(0)}=E^{(1)}\mathbf{C}^{(1)}+E^{(2)}\mathbf{C}^{(0)}, \tag{A6}$$

$$G_0\mathbf{C}^{(2)}+G_1\mathbf{C}^{(1)}+G_2\mathbf{C}^{(0)}=E^{(1)}\mathbf{C}^{(2)}+E^{(2)}\mathbf{C}^{(1)}+E^{(3)}\mathbf{C}^{(0)} \tag{A7}$$

$$\vdots$$

Here $\mathbf{C}^{(m)}$ is the vector

$$\begin{pmatrix} C_a^{(m)} \\ C_b^{(m)} \end{pmatrix} \tag{A8}$$

and the $\{G_i\}$ are 2×2 matrices evaluated in the degenerate subspace. More explicitly

$$G_0=\begin{pmatrix} V_{aa} & V_{ab} \\ V_{ba} & V_{bb} \end{pmatrix} \tag{A9}$$

while

$$G_1=\begin{pmatrix} \mathcal{R}^{\,1}_{aa} & \mathcal{R}^{\,1}_{ab} \\ \mathcal{R}^{\,1}_{ba} & \mathcal{R}^{\,1}_{bb} \end{pmatrix}, \tag{A10}$$

where $\mathcal{R}^{\,p}_{ij}\equiv\langle i|\mathcal{R}^{\,p}|j\rangle$ is the matrix element (i,j) of the operator

$$\mathcal{R}^{\,p}=\sum_i{}' \frac{V|i\rangle\langle i|V}{(E_a-E_i)^p}, \tag{A11}$$

and the prime indicates that the sum excludes the states $|a\rangle,|b\rangle$. In fact it is useful to define the more general operator

$$\mathcal{R}^{\,pq..r}=\sum_{i,j,..,k}{}' \frac{V|i\rangle\langle i|V|j\rangle\langle j|V\cdots V|k\rangle\langle k|V}{(E_a-E_i)^p(E_a-E_j)^q\cdots(E_a-E_k)^r}, \tag{A12}$$

and the operator $\Xi^m(l)$ as the sum over all the $\mathcal{R}$ operators with l superscripts such that they add up to m. For example,

$$\Xi^4(2)=\mathcal{R}^{\,13}+\mathcal{R}^{\,31}+\mathcal{R}^{\,22},$$

$$\Xi^5(3)=\mathcal{R}^{\,113}+\mathcal{R}^{\,131}+\mathcal{R}^{\,311}+\mathcal{R}^{\,122}+\mathcal{R}^{\,212}+\mathcal{R}^{\,221}. \tag{A13}$$

Further, we define the operator

$$\mathcal{M}^{\,m}_{\,l}=\Xi^m(l)-\sum_{j=1}^{l-1} E^{(j)}\mathcal{M}^{\,m+1-j}_{\,l-j}, \quad m,l\geqslant 2, \tag{A14}$$

with

$$\mathcal{M}^{\,m}_{\,1}=\Xi^m(1)=\mathcal{R}^{\,m}. \tag{A15}$$

For example, $\mathcal{M}^3_3$, from which we calculate G_3, is given by

$$\mathcal{M}^{\,3}_{\,3}=\mathcal{R}^{\,111}-E^{(1)}(\mathcal{R}^{\,12}+\mathcal{R}^{\,21}-E^{(1)}\mathcal{R}^{\,3})-E^{(2)}\mathcal{R}^{\,2}. \tag{A16}$$

Finally can write the matrices G_m as

$$G_m=\begin{pmatrix} \langle a|\mathcal{M}^{\,m}_{\,m}|a\rangle & \langle a|\mathcal{M}^{\,m}_{\,m}|b\rangle \\ \langle b|\mathcal{M}^{\,m}_{\,m}|a\rangle & \langle b|\mathcal{M}^{\,m}_{\,m}|b\rangle \end{pmatrix}. \tag{A17}$$

We can systematically solve the equations (A5)–(A7). However, in the problem investigated in this paper we have $V_{aa}=V_{ab}=V_{ba}=V_{bb}\equiv 0$ and thus $G_0=0$. Hence the first order energy corrections are zero ($E^{(1)}=0$), and we must use Eq. (A6) to determine the correct zero-order eigenstates and the energy corrections $E^{(2)}$. Equation (A6) is now a two-dimensional eigenvalue equation whose eigenvectors $\mathbf{C}^{(0)}_{\pm}$ and eigenvalues $E^{(2)}_{\pm}$ give the dressed states correct to zero-order and second-order energy corrections, respectively. Having found and normalized the eigenvectors $\mathbf{C}^{(0)}_{\pm}$, we proceed to solve Eq. (A7).

Because the matrices G_m are Hermitian, we know that the eigenvectors $\mathbf{C}^{(0)}_{\pm}$ are orthogonal and that they span the two-dimensional vector space. Therefore, we can write the vector $\mathbf{C}^{(1)}_{+}=f^{+}_{+}\mathbf{C}^{(0)}_{+}+f^{-}_{+}\mathbf{C}^{(0)}_{-}$. Substituting this back into Eq. (A7) and multiplying on the left first by $\mathbf{C}^{(0)^\dagger}_{+}$, then by $\mathbf{C}^{(0)^\dagger}_{-}$, we find

$$E^{(3)}_{+}=\mathbf{C}^{(0)^\dagger}_{+}G_2\mathbf{C}^{(0)}_{+}, \tag{A18}$$

$$f^{-}_{+}=\frac{1}{E^{(2)}_{+}-E^{(2)}_{-}}(\mathbf{C}^{(0)^\dagger}_{-}G_2\mathbf{C}^{(0)}_{+}).$$

The coefficient f^{+}_{+} is found to be arbitrary, and we choose $f^{+}_{+}=0$ in order to follow the orthogonality convention that

$${}^{(0)}\langle\psi|\psi\rangle^{(n)}=0. \tag{A19}$$

The previous derivation is symmetric and we can simply interchange plus and minus signs to obtain expressions for $E^{(3)}_{-}$ and f^{+}_{-}. The process can be continued to next order by taking $\mathbf{C}^{(2)}_{+}=g^{+}_{+}\mathbf{C}^{(0)}_{+}+g^{-}_{+}\mathbf{C}^{(0)}_{-}$, and so on. In this manner the energy corrections and coefficients of the degenerate states $C^{(n)}_a, C^{(n)}_b$ can be found to any accuracy required. The coefficients of the other states that contribute to the eigenvector corrections are found in the usual way, and given by

$$C^{(1)}_k=\frac{1}{E_a-E_k}(C^{(0)}_a V_{ka}+C^{(0)}_b V_{kb}), \tag{A20}$$

$$C^{(m)}_k=\frac{1}{E_a-E_k}\left(\sum_j C^{(m-1)}_j V_{kj}-\sum_{i=1}^{m-1} E^{(i)}C^{(m-i)}_k\right),$$

where we point out that the first sum includes the states $|a\rangle,|b\rangle$.

APPENDIX B: TRANSITION RATES BETWEEN THE DRESSED STATES

For $n=2$ the transition rates (20) to order α^2 are given by

$$\begin{aligned}
&\Gamma_{-3}^{\pm\pm}=\frac{1}{13}\,\alpha^2, && \Gamma_{-3}^{\pm\mp}=\left(\frac{17}{117}\pm\frac{4\sqrt{13}}{117}\right)\alpha^2,\\
&\Gamma_{-2}^{\pm\pm}=\frac{9}{208}-\frac{1405}{5408}\,\alpha^2, && \Gamma_{-2}^{\pm\mp}=\frac{17}{208}\pm\frac{\sqrt{13}}{52}-\left(\frac{17099}{48672}\mp\frac{6803\sqrt{13}}{97344}\right)\alpha^2,\\
&\Gamma_{-1}^{\pm\pm}=\frac{13}{36}\,\alpha^2, && \Gamma_{-1}^{\pm\mp}=\frac{1}{4}\,\alpha^2,\\
&\Gamma_{0}^{\pm\pm}=\frac{1}{13}-\frac{2201}{12168}\,\alpha^2, && \Gamma_{0}^{\pm\mp}=\frac{9}{52}-\left(\frac{131}{1352}\mp\frac{3\sqrt{13}}{26}\right)\alpha^2,\\
&\Gamma_{1}^{\pm\pm}=\frac{4}{117}\,\alpha^2, && \Gamma_{1}^{\pm\mp}=\frac{1}{13}\,\alpha^2,\\
&\Gamma_{2}^{\pm\pm}=\frac{9}{208}-\frac{261}{5408}\,\alpha^2, && \Gamma_{2}^{\pm\mp}=\frac{17}{208}\mp\frac{\sqrt{13}}{52}-\left(\frac{3059}{48672}\mp\frac{1187\sqrt{13}}{97344}\right)\alpha^2,\\
&\Gamma_{3}^{\pm\pm}=\frac{1}{52}\,\alpha^2, && \Gamma_{3}^{\pm\mp}=\left(\frac{17}{468}\mp\frac{\sqrt{13}}{117}\right)\alpha^2.
\end{aligned}\tag{B1}$$

The left-hand column of Eq. (B1) consists of those transition rates which contribute to the central components of the fluorescence triplets, the right-hand column are transition rates which govern the intensities of the triplet sidebands. For $n=3$ we find the transition rates correct to order α^4 to be given by

$$\begin{aligned}
&\Gamma_{0}^{\pm\pm}=\frac{1}{4}-\frac{369}{256}\,\alpha^2+\frac{4844169}{409600}\,\alpha^4, && \Gamma_{0}^{+-}=\frac{81}{64}\,\alpha^2-\frac{26163}{2560}\,\alpha^4, && \Gamma_{0}^{-+}=\frac{81}{64}\,\alpha^2-\frac{18549}{1280}\,\alpha^4,\\
&\Gamma_{1}^{\pm\pm}=\frac{81}{1024}\,\alpha^2-\frac{45927}{65536}\,\alpha^4, && \Gamma_{1}^{+-}=\frac{6561}{16384}\,\alpha^4, && \Gamma_{1}^{-+}=\frac{3969}{4096}\,\alpha^4,\\
&\Gamma_{-1}^{\pm\pm}=\frac{81}{1024}\,\alpha^2+\frac{325053}{327680}\,\alpha^4, && \Gamma_{-1}^{+-}=\frac{6561}{4096}\,\alpha^4, && \Gamma_{-1}^{-+}=\frac{6561}{16384}\,\alpha^4,\\
&\Gamma_{2}^{\pm\pm}=\frac{263169}{409600}\,\alpha^4, && \Gamma_{-2}^{+-}=\frac{81}{64}\,\alpha^2-\frac{485757}{40960}\,\alpha^4, && \Gamma_{2}^{-+}=\frac{9}{64}\,\alpha^2-\frac{50949}{40960}\,\alpha^4,\\
&\Gamma_{-2}^{\pm\pm}=\frac{927369}{409600}\,\alpha^4, && \Gamma_{3}^{+-}=\frac{6561}{16384}\,\alpha^4, && \Gamma_{3}^{-+}=\frac{1}{4}-\frac{597}{512}\,\alpha^2+\frac{55103607}{6553600}\,\alpha^4,\\
&\Gamma_{3}^{\pm\pm}=\frac{81}{256}\,\alpha^2-\frac{677889}{163840}\,\alpha^4, && \Gamma_{-3}^{+-}=\frac{1}{4}-\frac{1365}{512}\,\alpha^2+\frac{125778807}{6553600}\,\alpha^4, && \Gamma_{-3}^{-+}=\frac{6561}{16384}\,\alpha^4,\\
&\Gamma_{-3}^{\pm\pm}=\frac{81}{256}\,\alpha^2-\frac{207117}{32768}\,\alpha^4, && \Gamma_{-4}^{+-}=\frac{225}{256}\,\alpha^2-\frac{89343}{16384}\,\alpha^4, && \Gamma_{4}^{-+}=\frac{81}{256}\,\alpha^2-\frac{105219}{81920}\,\alpha^4,\\
&\Gamma_{4}^{\pm\pm}=\frac{6561}{16384}\,\alpha^4, && \Gamma_{-5}^{+-}=\frac{3538161}{6553600}\,\alpha^4, && \Gamma_{5}^{-+}=\frac{6561}{16384}\,\alpha^4,\\
&\Gamma_{-4}^{\pm\pm}=\frac{18225}{16384}\,\alpha^4, &&&&
\end{aligned}\tag{B2}$$

while for $n=4$ we find to order α^4

$$\Gamma_0^{\pm\pm}=\frac{1}{4}-\frac{34}{225}\alpha^2-\frac{149486}{50625}\alpha^4,\quad \Gamma_0^{+-}=\frac{25}{9}\alpha^4,\quad \Gamma_0^{-+}=\frac{25}{9}\alpha^4,$$

$$\Gamma_1^{\pm\pm}=\frac{16}{225}\alpha^2-\frac{3136}{50625}\alpha^4,\quad \Gamma_{-2}^{+-}=\frac{400}{81}\alpha^4,\quad \Gamma_2^{-+}=\frac{4}{81}\alpha^4,$$

$$\Gamma_{-1}^{\pm\pm}=\frac{16}{225}\alpha^2+\frac{4064}{50625}\alpha^4,\quad \Gamma_{-3}^{+-}=\frac{16}{9}\alpha^2-\frac{28288}{2025}\alpha^4,\quad \Gamma_3^{-+}=\frac{4}{9}\alpha^2-\frac{2272}{2025}\alpha^4,$$

$$\Gamma_2^{\pm\pm}=\frac{16}{225}\alpha^4,\quad \Gamma_{-4}^{+-}=\frac{1}{4}-\frac{707}{225}\alpha^2+\frac{1463321}{101250}\alpha^4,\quad \Gamma_4^{-+}=\frac{1}{4}-\frac{257}{225}\alpha^2+\frac{95321}{101250}\alpha^4,$$

$$\Gamma_{-2}^{\pm\pm}=\frac{4}{225}\alpha^4,\quad \Gamma_{-5}^{+-}=\frac{36}{25}\alpha^2-\frac{15392}{1875}\alpha^4,\quad \Gamma_5^{-+}=\frac{16}{25}\alpha^2-\frac{1024}{625}\alpha^4,$$

$$\Gamma_4^{\pm\pm}=\frac{25}{36}\alpha^4,\quad \Gamma_{-6}^{+-}=\frac{8836}{5625}\alpha^4,\quad \Gamma_6^{-+}=\frac{1936}{5625}\alpha^4,$$

$$\Gamma_{-4}^{\pm\pm}=\frac{25}{36}\alpha^4. \tag{B3}$$

In Eqs. (B2) and (B3) the left-hand column consists of those transition rates corresponding to the central components of the fluorescence triplets, the middle and right columns correspond to right and left sidebands of the triplets, respectively. An examination of Eqs. (B2) and (B3) reveals that the only transition rates that have nonvanishing terms independent of α are $\Gamma_0^{\pm\pm}$, which correspond to transitions at ω_0, and $\Gamma_{\mp n}^{\pm\mp}$, which correspond to sidebands of the triplets at $\pm 2\Omega_1$, the location of the Rabi sidebands for monochromatic driving.

The quantities (44), which determine the intensities of the Autler-Townes spectral lines, are found to be as follows: For $n=2$:

$$\Lambda_{-1}^{\pm}=\left(\frac{1}{9}\mp\frac{2\sqrt{13}}{117}\right)\alpha^2,$$

$$\Lambda_0^{\pm}=\left(\frac{1}{4}\mp\frac{\sqrt{13}}{26}\right)-\left(\frac{5}{18}\mp\frac{433\sqrt{13}}{48672}\right)\alpha^2,$$

$$\Lambda_2^{\pm}=\left(\frac{1}{4}\pm\frac{\sqrt{13}}{26}\right)-\left(\frac{1}{9}\pm\frac{1993\sqrt{13}}{48672}\right)\alpha^2,$$

$$\Lambda_1^{\pm}=\left(\frac{1}{4}\mp\frac{\sqrt{13}}{26}\right)\alpha^2.$$

For $n=3$:

$$\Lambda_0^{+}=\frac{81}{128}\alpha^2-\frac{1215081}{163840}\alpha^4,$$

$$\Lambda_0^{-}=\frac{1}{2}-\frac{825}{512}\alpha^2+\frac{27429651}{3276800}\alpha^4,$$

$$\Lambda_1^{+}=\frac{729}{512}\alpha^4,\quad \Lambda_1^{-}=\frac{81}{128}\alpha^2-\frac{81405}{32768}\alpha^4,$$

$$\Lambda_{-1}^{+}=\frac{18225}{32768}\alpha^4,\quad \Lambda_{-1}^{-}=\frac{225}{512}\alpha^2-\frac{130923}{131072}\alpha^4,$$

$$\Lambda_2^{+}=\frac{9}{128}\alpha^2-\frac{25893}{32768}\alpha^4,\quad \Lambda_2^{-}=\frac{729}{512}\alpha^4, \tag{B4}$$

$$\Lambda_3^{+}=\frac{1}{2}-\frac{489}{512}\alpha^2+\frac{19169811}{3276800}\alpha^4,\quad \Lambda_{-2}^{-}=\frac{35721}{819200}\alpha^4,$$

$$\Lambda_4^{+}=\frac{81}{512}\alpha^2-\frac{41067}{131072}\alpha^4,\quad \Lambda_3^{-}=\frac{81}{128}\alpha^2-\frac{962361}{163840}\alpha^4,$$

$$\Lambda_5^{+}=\frac{6561}{819200}\alpha^4,\quad \Lambda_4^{-}=\frac{6561}{32768}\alpha^4.$$

For $n=4$:

$$\Lambda_0^{+}=\frac{25}{18}\alpha^4,\quad \Lambda_0^{-}=\frac{1}{2}-\frac{347}{225}\alpha^2+\frac{27821}{33750}\alpha^4,$$

$$\Lambda_3^{+}=\frac{2}{9}\alpha^2-\frac{196}{675}\alpha^4,\quad \Lambda_1^{-}=\frac{8}{9}\alpha^2-\frac{1424}{675}\alpha^4,$$

$$\Lambda_4^{+}=\frac{1}{2}-\frac{137}{225}\alpha^2-\frac{32099}{33750}\alpha^4,\quad \Lambda_{-1}^{-}=\frac{18}{25}\alpha^2-\frac{644}{625}\alpha^4,$$

$$\Lambda_5^{+}=\frac{8}{25}\alpha^2-\frac{1616}{5625}\alpha^4,\quad \Lambda_2^{-}=\frac{8}{9}\alpha^4,$$

$$\Lambda_6^{+}=\frac{8}{225}\alpha^4,\quad \Lambda_{-2}^{-}=\frac{32}{225}\alpha^4,\quad \Lambda_4^{-}=\frac{25}{18}\alpha^4.$$

These are correct to order α^2 for $n=2$, and order α^4 for $n=3,4$.

[1] B. R. Mollow, Phys. Rev. **188**, 1969 (1969).
[2] F. Schuda, C. R. Stroud, Jr., and M. Hercher, J. Phys. B **7**, L198 (1974); F. Y. Wu, R. E. Grove, and S. Ezekiel, Phys. Rev. Lett. **35**, 1426 (1975).
[3] B. R. Mollow, Phys. Rev. A **5**, 2217 (1972); F. Y. Wu, S. Ezekiel, M. Ducloy, and B. R. Mollow, Phys. Rev. Lett. **38**, 1077 (1977); C. Wei and N. B. Manson, Phys. Rev. A **49**, 4751 (1994); A. D. Wilson-Gordon and H. Friedmann, Opt. Commun. **94**, 238 (1992); Tran Quang and Helen Freedhoff, Phys. Rev. A **48**, 3216 (1993).
[4] S. H. Autler and C. H. Townes, Phys. Rev. **100**, 703 (1955); C. Wei, N. B. Manson, and J. P. D. Martin, Phys. Rev. A **51**, 1438 (1995).
[5] Y. Zhu, A. Lezama, D. J. Gauthier, and T. W. Mossberg, Phys. Rev. A **41**, 6574 (1990).
[6] H. S. Freedhoff and Z. Chen, Phys. Rev. A **41**, 6013 (1990); **46**, 732(E) (1992).
[7] G. Kryuchkov, Opt. Commun. **54**, 19 (1985); S. P. Tewari and M. K. Kumari, Phys. Rev. A **41**, 5273 (1990); G. S. Agarwal, Y. Zhu, D. J. Gauthier, and T. W. Mossberg, J. Opt. Soc. Am. B **8**, 1163 (1991).
[8] Z. Ficek and H. S. Freedhoff, Phys. Rev. A **48**, 3092 (1993), and references therein.
[9] M. F. Van Leeuwen, S. Papademetriou, and C. R. Stroud, Jr., Phys. Rev. A **53**, 990 (1996); S. Papademetriou, M. F. Van Leeuwen, and C. R. Stroud, Jr., *ibid.* **53**, 997 (1996).
[10] N. B. Manson, C. Wei, and J. P. D. Martin, Phys. Rev. Lett. **76**, 3943 (1996), and references therein.
[11] S. Feneuille, M. G. Scheighofer, and G. Oliver, J. Phys. B **9**, 2003 (1976); A. M. Bonch-Bruevich, T. A. Vartanyan, and N. A. Chigir, Zh. Eksp. Teor. Fiz. **77**, 1899 (1979) [Sov. Phys. JETP **50**, 901 (1979)]; P. Thomann, J. Phys. B **13**, 1111 (1980); G. S. Agarwal and N. Nayak, J. Opt. Soc. Am. B **1**, 164 (1984); H. Friedmann and A. D. Wilson-Gordon, Phys. Rev. A **36**, 1333 (1987); S. Chakmakjian, K. Koch, and C. R. Stroud, Jr., J. Opt. Soc. Am. B **5**, 2015 (1988).
[12] S. Papademetriou, S. M. Chakmakjian, and C. R. Stroud, Jr., J. Opt. Soc. Am. B **9**, 1182 (1992).
[13] B. Lounis, F. Jelezko, and M. Orrit, Phys. Rev. Lett. **78**, 3673 (1997).
[14] Y. Zhu, Q. Wu, S. Morin, and T. Mossberg, Phys. Rev. Lett. **65**, 1200 (1990).
[15] D. J. Gauthier, Q. Wu, E. S. Morin, and T. W. Mossberg, Phys. Rev. Lett. **68**, 464 (1992).
[16] J. R. Ackerhalt and B. W. Shore, Phys. Rev. A **16**, 277 (1977); R. M. Whitley and C. R. Stroud, Jr., *ibid.* **14**, 1498 (1976); R. Salomaa, J. Phys. B **10**, 3005 (1977); L. Allen and C. R. Stroud, Jr., Phys. Rep. **91**, 1 (1982).
[17] G. Grynberg and C. Cohen-Tannoudji, Opt. Commun. **96**, 150 (1993).
[18] P. B. Sellin, C. C. Yu, J. R. Bochinski, and T. W. Mossberg, Phys. Rev. Lett. **78**, 1432 (1997).
[19] C. Cohen-Tannoudji and S. Reynaud, J. Phys. B **10**, 345 (1977); C. Cohen-Tannoudji, J. Dupont-Roc, and G. Grynberg, *Atom-Photon Interactions* (Wiley, New York, 1992).
[20] G. S. Agarwal, in *Quantum Optics*, edited by G. Höhler, Springer Tracts in Modern Physics Vol. 70 (Springer, Berlin, 1974), p. 25.
[21] Z. Ficek and H. S. Freedhoff, Phys. Rev. A **53**, 4275 (1996).
[22] C. C. Yu, J. R. Bochinski, T. M. V. Kordich, T. W. Mossberg, and Z. Ficek, Phys. Rev. A **56**, R4381 (1997).
[23] K. Catchpole, A. Greentree, C. Wei, S. Holstrom, N. Manson, and J. Martin, in *Proceedings of the International Quantum Electronics Conference, 1996* (Optical Society of America, Washington, D.C., 1996), p. 203.
[24] M. Lax, Phys. Rev. **172**, 350 (1968).
[25] M. O. Scully, Phys. Rev. Lett. **67**, 1855 (1991); M. O. Scully and M. Fleischhauer, *ibid.* **69**, 1360 (1992); A. D. Wilson-Gordon and H. Friedmann, Opt. Commun. **94**, 238 (1992); T. Quang and H. S. Freedhoff, Phys. Rev. A **48**, 3216 (1993); C. Szymanowski and C. H. Keitel, J. Phys. B **27**, 5795 (1994).